Rapid Catalytic Oxygenation of Hydrocarbons by Ruthenium Pentafluorophenylporphyrin Complexes: Evidence for the Involvement of a Ru(III) Intermediate

John T. Groves,* Marcella Bonchio,† Tommaso Carofiglio,‡ and Kirill Shalyaev

Department of Chemistry, Princeton University Princeton, New Jersey 08544

Received December 15, 1995

New methods for the catalytic oxygenation of hydrocarbons continue to be of fundamental interest[1] and potential economic value.[2] Among the metalloporphyrin-mediated oxidations,[1,3] ruthenium catalysts display remarkable activity for aerobic oxidations[3b,4] and promising reactivity with N_2O.[5] Recently, Hirobe et al.[6] have reported efficient oxygenation reactions with ruthenium porphyrin complexes and aromatic *N*-oxides in the presence of strong mineral acids. Here we describe the very rapid oxygenation of a variety of substrates including alkanes, terminal olefins, and benzene, catalyzed by perfluorinated ruthenium porphyrin complexes[7] in aprotic media and a dissection of the mechanism of this process.

Carbonyl (5,10,15,20-tetrapentafluorophenylporphyrinato)-ruthenium(II) [Ru^{II}(TPFPP)(CO)], **1**,[8] has shown remarkable activity[9] with 2,6-dichloropyridine-*N*-oxide [$pyCl_2NO$] as the oxygen donor. Hydroxylations of adamantane and *cis*-decalin were achieved with high selectivity, complete stereoretention, high rates (up to 800 turnovers/min), and high efficiency (400−14600 turnovers, Table 1, entries 1−3). Oxygenation of less reactive substrates proceeded with lower but still significant turnover numbers (100−3000, Table 1, entries 4, 5, and 7).[10]

Analysis of the adamantane hydroxylation catalyzed by **1** provided revealing information with respect to the mechanism. The evolution of products over time (curve A, Figure 1) showed an initial induction period followed by a fast, zero-order phase with maximum rate and the highest efficiencies (column 6, Table 1). Deviation from linear behavior was observed only after 90% of the oxygen donor and 80% of the substrate had been consumed. Recharge of the reaction mixture with $pyCl_2NO$ and adamantane afforded another catalytic burst with a similar rate but with no induction period (curve B, Figure 1). Thus, the active form of the catalyst was still fully efficient.

Table 1. Hydrocarbon Oxidation[a] Catalyzed by [Ru^{II}TPFPP)(CO)]

No.	substrate	time (min)	product (% conv.)[b]	yield[c] (%)	max rate[d] (turnovers/min)
1[e]	adamantane	20	1-adamantanol (76.2) adamantane-1,3-diol (7.3)	91	72
2[f]	adamantane	120	1-adamantanol (61.0) adamantane-1,3-diol (6.0)	97	800
3	*cis*-decalin	25	(*Z*)-9-decalol (79.6) (*Z*)-decal-9,10-diol (4.2)	90	64
4	*trans*-decalin	60	(*E*-9-decalol (25.8) secondary alcohols (4.3) ketones (13.9)	70	4.4
5[f]	cyclohexane	180	cyclohexanol (1.6) cyclohexanone (6.7)	95	22
6	1-octene	60	1,2-epoxyoctane (96)	96	11 (36)[g]
7	1-octene/ adamantane	60	1,2-epoxyoctane (54) 1-adamantanol (28)	90	9.5 4.8
8[h]	benzene	12h	1,4-benzoquinone (13.3)	40	

[a] [substrate] = [$pyCl_2NO$] = 0.02 M, [**1**] = 50 μM. All reactions in CH_2Cl_2 at 65 °C in sealed containers. No difference was registered in reactions performed under aerobic or anaerobic conditions. [b] Percent conversion based on substrate consumed. Products were identified by GC−MS and compared to authentic samples. [c] Percent yield based on $pyCl_2NO$ consumed. [d] Maximum oxidation rate measured as the slope of the zero-order phase of the kinetic plot (see text). Turnover numbers based on the substrate conversion. [e] Similar conversions were obtained with [Ru^{VI}(TPFPP)$(O)_2$][18−22] and [Ru^{VI}(TPFPBr$_8$P)$(O)_2$][21] with $pyCl_2NO$. [f] [substrate] = [$pyCl_2NO$] = 0.2 M, [**1**] = 10 μM. [g] Cf. ref 16. [h] [benzene] = 2 M, [$pyCl_2NO$] = 0.02 M, [**1**] = 50 μM.

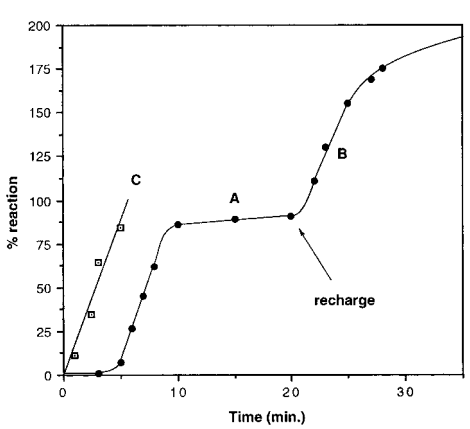

Figure 1. Time course for adamantane hydroxylation by **1** in CH_2Cl_2 at 65 °C; adamantane (0.02 M), $pyCl_2NO$ (0.02 M), **1** (50 μM); 1-adamantanol determined by GC (±1%). Curve A: typical kinetic trace with **1** as catalyst, $r = 0.999$ for the linear section, 68 ± 4 turnovers/min for triplicate runs. Curve B: reaction A recharged with $pyCl_2NO$ and adamantane to 0.02 M at $t = 20$ min. Curve C: **4a** used as the catalyst (see text).

The transformation of **1** to the active catalyst proceeded *via* an adduct **2** [$K = 350$ M^{-1}, at 25 °C], as detected by changes in the IR (1959−1950 cm^{-1}) and UV−vis (404−406 nm) spectra. Photostimulation with red-orange light (>560 nm) was observed,[11] consistent with photoejection of the carbonyl ligand.

Ruthenium porphyrin radical cations are known to be formed from the corresponding carbonyl compounds by chemical or electrochemical oxidation.[12] Further, these species show a characteristic absorption band in the 600−700 nm region.[12c] The radical cation **3** was quantitatively generated by reaction of **1** with ferric perchlorate.[13] The shift of ν CO (from 1950 to 1979 cm^{-1}), the broadening of the Soret band, the appearance of a

* Author to whom correspondence should be addressed.
† Current address: Dipartimento di Chimica Organica, Università di Padova, Italy.
‡ Current address: Dipartimento di Chimica Inorganica, Metallorganica ed Analitica, Università di Padova, Italy.

(1) (a) Groves, J. T.; Han, Y.-Z. In *Cytochrome P-450. Structure, Mechanism and Biochemistry*; Ortiz de Montellano, P. R., Ed.; Plenum Press: New York, 1995; pp 3−48. (b) Groves, J. T.; Nemo, T. E. *J. Am. Chem. Soc.* **1983**, *105*, 6243−6248. (c) *Activation and functionalization of alkanes*; Hill, C. L., Ed.; John Wiley & Sons: New York, 1989.

(2) *Selective Hydrocarbon Activation: Principle and Progress*; Davies, J. A., et al., Eds; VCH: New York, 1994.

(3) (a) *Metalloporphyrins in Catalytic Oxidations*; Sheldon, R. A., Ed.; M. Dekker: New York, 1994. (b) Mlodnika, T.; James, B. R. In *Metalloporphyrin Catalyzed Oxidations*; Montanari, F., Casella, L., Eds.; Kluwer: Dordrecht, The Netherlands, 1994; p 121.

(4) (a) Groves, J. T.; Quinn, R. *Inorg. Chem.* **1984**, *23*, 3844−3846. (b) Groves, J. T.; Quinn, R. *J. Am. Chem. Soc.* **1985**, *107*, 5790−5792. (c) Groves, J. T.; Ahn, K.-H. *Inorg. Chem.* **1987**, *26*, 3831−3833. (d) Groves, J. T.; Quinn, R. U.S. Patent 4,822,899, April 18, 1989.

(5) Groves, J. T.; Roman, J. S. *J. Am. Chem. soc.* **1995**, *117*, 5594−5595.

(6) (a) Higuchi, T.; Satake, C.; Hirobe, M. *J. Am. Chem. Soc.* **1995**, *117*, 8879−8880. (b) Ohtake, H.; Higuchi, T.; Hirobe, M. *Heterocycles* **1995** and references therein. (c) Higuchi, T. *J. Synth. Org. Chem. Jpn.* **1995**, *53*, 644−644.

(7) (a) Ellis, P. E.; Lyons, J. E. *Coord. Chem. Rev.* **1990**, *105*, 181−193. (b) Birnbaum, E. R.; Schaefer, W. P.; Labinger, J. A.; Bercaw, J. E., Gray, H. B. *Inorg. Chem.* **1995**, *34*, 1751−1755. (c) Murahashi, S.-I.; Naota, T.; Komiya, N. *Tetrahedron Lett.* **1995**, *36*, 8059−8062.

(8) **1** was prepared by metalation of the free base with $Ru_3(CO)_{12}$ in refluxing *o*-dichlorobenzene (55% yield). ^{1}H-NMR ($CDCl_3$, δ) 8.70. IR (KBr, cm^{-1}) 1965 (ν C═O). UV−vis ($CHCl_3$, nm) 404, 524, 554. Cf. ref 7c.

(9) Vis-à-vis Ru^{VI}-dioxo and Ru^{IV}-oxo porphyrin based systems (cf. ref 4 and Ho, C.; Leung, W.-H.; Che, C.-M. *J. Chem. Soc., Dalton Trans.* **1991**, 2933−2939.)

(10) Degradation of the active catalyst at higher catalyst concentration, which is more pronounced with the less reactive substrates, would account for the high activity at lower catalyst concentration (Table 1, entry 2). Also the identity of the axial ligand X, in Scheme 1, is probably concentration dependent, thus further affecting the reaction rates.

(11) Unfiltered irradiation (tungsten lamp, 300 W) caused the rapid degradation of the porphyrin ligand.

S0002-7863(95)04209-0 CCC: $12.00

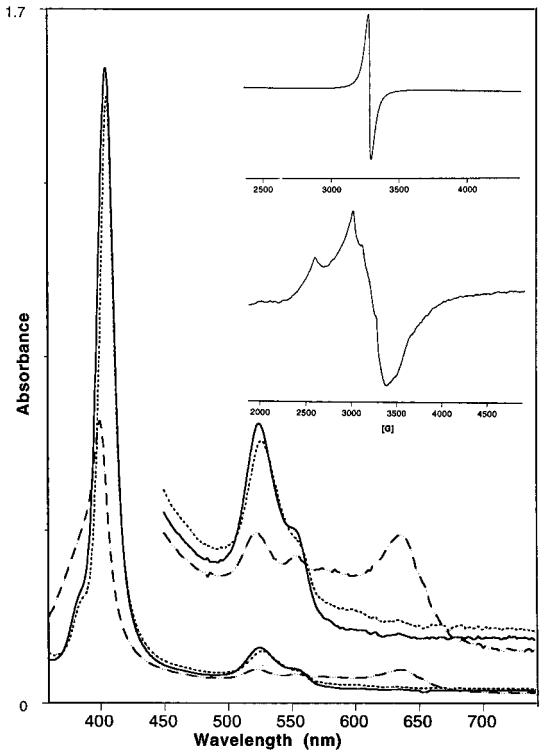

Figure 2. Superimposed UV spectra (CH_2Cl_2, 25 °C) of **2** (—) (**1** = [50 μM] + $pyCl_2NO$ = [0.02 M]), **3** (– · –), and **4a** (· · ·). Inset: X-band EPR of **3** (inset a) and **4b** (inset b) recorded in CH_2Cl_2 at 135 K.

635 nm absorption (Figure 2, dotted curve), and the EPR signal ($g = 2.00$) (Figure 2, inset a) agree with the proposed structure for **3**.[12c] Dichloromethane solutions of compound **3** were stable at low temperature, but **3** converted slowly to **1** with clean isosbestic behavior (IR and UV−vis) upon standing at 25 °C.

Reaction of **3** with an excess of the *N*-oxide at −50 °C induced a color change from green to orange. Evolution of CO was observed as the solution reached 25 °C, leading to species **4a** (Figure 2, line-dotted curve). The occurrence of an internal electron transfer process from ruthenium(II) to the porphyrin radical cation upon ligation has been reported.[12c] Indeed, compound **4b** (OD = 2,6-lutidine-*N*-oxide) showed an EPR signal typical of a ruthenium(III) species[12d,e] (Figure 2, inset b, $g_\perp = 2.55$, $g_{||} = 2.05$). Significantly, compound **4a** (OD = $pyCl_2NO$) catalyzed adamantane hydroxylation with no induction period.[14] However, the zero-order regime occurred with a similar rate (Figure 1, curve C). Moreover, **4a** was the species observed by UV−vis spectroscopy during the rapid phase of catalysis.

On the basis of the above observations, we propose the catalytic cycle in Scheme 1 for this reaction. Such a mechanism accounts both for the slow initiation leading to the formation of **4a** and for the zero-order phase of the oxygenation process. Significantly, the hydroxylation of adamantane showed a kinetic deuterium isotopic effect (k_H/k_D = 3.05 at 65 °C) in a competitive experiment, while deuterated and undeuterated

Scheme 1

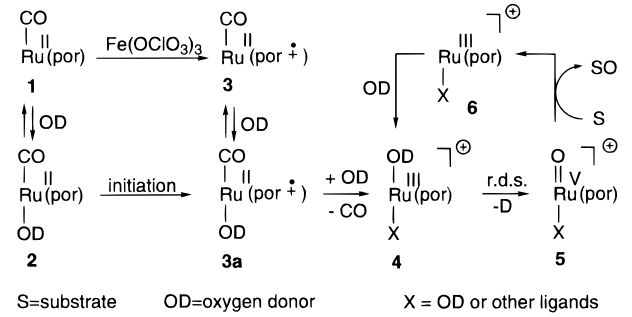

substrates displayed the *same rate* in the fast kinetic phase in separate reactions. Similar results were obtained for decalin (k_H/k_D = 5.4 at 40 °C). These observations can be explained if a reactive intermediate, such as **5**, is formed *in the rate-determining step*. The temperature dependence of adamantane hydroxylation suggested a significant barrier for the N−O bond cleavage step.[15]

The unusually low reactivity of 1-octene with respect to adamantane and *cis*-decalin appeared to result from catalyst inhibition by this substrate. Thus, 1-octene was twice as reactive as adamantane in competitive oxidation, and the efficiency of the 1-octene epoxidation was improved 3-fold when excess $pyCl_2NO$ was employed.[16] Coordination of 1-octene to the Ru^{III} center would explain this observation, but no such adduct was observed.[17]

The results are consistent with the rate-determining formation of a Ru^{V}-oxo species or a Ru^{IV}-oxo porphyrin radical cation[12a,b] (**5**) as the reactive species in these reactions. A similar transformation of a Ru^{III} octaethyl porphyrin (OEP) complex to a reactive oxo-Ru^{IV} (OEP) cation radical has been proposed by Dolphin and James;[3b,12a,b] however, the stability reported for that species at 25°[12f] stands in contrast to the reactivity of **5**. Significantly, $pyCl_2NO$ was not able to oxidize [Ru^{IV}(TPFPP)(O)] to [Ru^{VI}(TPFPP)$(O)_2$][18] rapidly, and this oxidant is an unlikely intermediate.[19] Oxygen donors such as iodosylbenzene, magnesium monoperoxyphthalate, oxone, and tetrabutylammonium periodate were able to produce the *trans*-dioxo species but were ineffective for rapid catalysis under the conditions described here.[20]

Rapid, efficient hydrocarbon oxygenation can be achieved with a perfluorophenyl Ru^{III} porphyrin catalyst *via* the stepwise oxidation of the ruthenium(II) carbonyl complex. A search for accesses to the key Ru^{III}−Ru^{V} cycle from O_2, N_2O, and H_2O_2 is underway.

Acknowledgment. Support of the National Science Foundation and fellowship grants to M.B. and T.C. from the University of Padova are gratefully acknowledged.

JA9542092

(12) (a) Dolphin, D.; James, B. R.; Leung, T. *Inorg. Chim. Acta* **1983**, *79*, 25−27. (b) Leung, T.; James, B. R.; Dolphin, D. *Inorg. Chim. Acta* **1983**, *79*, 180−181. (c) Barley, M.; Becker, J. Y.; Domazetis, G.; Dolphin, D.; James, B. R. *Can. J. Chem.* **1983**, *61*, 2389−2396. (d) James, B. R.; Dolphin, D.; Leung, T. W.; Einstein, F. W.; Willis, A. C. *Can. J. Chem.* **1984**, *62*, 1238−1245. (e) James, B. R.; Mikkelsen, S. R.; Leung, T. W.; Williams, G. M., Wong, R. *Inorg. Chim. Acta B* **1984**, *85*, 209−213. (f) For a review, see: James, B. R. In *Fundamentals of Research in Homogeneous Catalysis*; Shilov, A. E., Ed. Gordon Breach: New York, 1986; pp 309−324.

(13) An emerald green solution of **3** was obtained upon oxidation of **1** with $Fe(ClO_4)_3 \cdot nH_2O$ in CH_2Cl_2; IR (CH_2Cl_2, −50 °C,) 1979 cm^{-1} (ν C═O).

(14) $PyCl_2NO$ was added to a solution of **3** at −50 °C. The substrate was added after **4a** formed at 25 °C. The reaction mixture was then heated at 65 °C.

(15) An Eyring plot of the zero-order rate constants determined over the range 318−338 K was linear indicating a $\Delta H^{\ddagger}$ of 28.6 kcal/mol and a small but positive $\Delta S^{\ddagger}$ of 7.0 cal mol^{-1} K^{-1}; (ln k = −9.73, −10.76, −12.39 at 338, 328, and 318 K, respectively).

(16) [1-octene] = 0.01 M, [$pyCl_2NO$] = 0.04 M, [**1**] = 50 μM, in CH_2Cl_2 at 65 °C, maximum rate = 36 turnovers/min (entry 6, Table 1).

(17) Groves, J. T.; Ahn, K.-H.; Quinn, R. *J. Am. Chem. Soc.* **1988**, *110*, 4217−4220.

(18) [Ru^{VI}(TPFPP)$(O)_2$] was obtained by oxidation of **1** with *m*-chloroperbenzoic acid (*m*-CPBA) in CH_2Cl_2. ^{1}H-NMR ($CDCl_3$, δ) 9.16. IR (KBr, cm^{-1}) 826 (ν Ru═O). UV−vis ($CHCl_3$, nm) 412, 506. Ru^{IV}(TPFPP)(O) was prepared from [Ru^{VI}(TPFPP)$(O)_2$] by treatment with PPh_3[17]. ^{1}H-NMR ($CDCl_3$, δ) −8.70. Excess $pyCl_2NO$ did not afford [Ru^{VI}(TPFPP)$(O)_2$] in 48 h.

(19) No products were observed upon spontaneous decomposition of [Ru^{VI}(TPFPP)$(O)_2$] in the presence of adamantane.

(20) The hydroxylation of steroids and similar substrates was observed when [Ru^{VI}(TPFPP)$(O)_2$] was used as starting catalyst in the presence of $pyCl_2NO$; however, turnover was slower, and no variation of the UV−vis spectrum of [Ru^{VI}(TPFPP)$(O)_2$] was observed during catalysis.

(21) [Ru^{VI}(TPFPBr$_8$P)$(O)_2$] was obtained by oxidation of the corresponding Ru(II)−carbonyl complex[7b] with *m*-CPBA in CH_2Cl_2. IR (KBr, cm^{-1}) 830 (ν Ru═O), UV−vis ($CHCl_3$, nm) 440, 524, 560.